

Target Gene Specificity of USF-1 Is Directed via p38-mediated Phosphorylation-dependent Acetylation*

Received for publication, November 12, 2008, and in revised form, March 26, 2009 Published, JBC Papers in Press, April 23, 2009, DOI 10.1074/jbc.M808605200

Sébastien Corre^{‡§1}, Aline Primot[§], Yorann Baron[§], Jacques Le Seyec[¶], Colin Goding^{‡||},
and Marie-Dominique Galibert^{§2}

From the [‡]Signaling and Development Laboratory, Marie Curie Research Institute, The Chart, Oxted RH8 OTL, United Kingdom, [§]CNRS UMR 6061, Genetic and Development Institute of Rennes, Régulation Transcriptionnelle et Oncogénèse Team, Université de Rennes-1, Faculté de Médecine, Institut Fédérative de Recherche (IFR) 140 Génomique Fonctionnelle Agronomique et Santé (GFAS), 2 Avenue du Professor Léon Bernard, CS 34317, Rennes 35043 Cedex, France, [¶]INSERM U522, Hôpital Pontchaillou, IFR140 GFAS, Avenue Henri Le Guilloux, Rennes 35033 Cedex, France, and the ^{||}Ludwig Institute for Cancer Research, University of Oxford, Old Road Campus Research Building, Old Road Campus, Headington, Oxford OX3 7DQ, United Kingdom

How transcription factors interpret the output from signal transduction pathways to drive distinct programs of gene expression is a key issue that underpins development and disease. The ubiquitously expressed basic-helix-loop-helix leucine zipper upstream stimulating factor-1 binds E-box regulatory elements (CANNTG) to regulate a wide number of gene networks. In particular, USF-1 is a key component of the tanning process. Following UV irradiation, USF-1 is phosphorylated by the p38 stress-activated kinase on threonine 153 and directly up-regulates expression of the *POMC*, *MC1R*, *TYR*, *TYRP-1* and *DCT* genes. However, how phosphorylation on Thr-153 might affect the activity of USF-1 is unclear. Here we show that, in response to DNA damage, oxidative stress and cellular infection USF-1 is acetylated in a phospho-Thr-153-dependent fashion. Phospho-acetylated USF-1 is nuclear and interacts with DNA but displays altered gene regulatory properties. Phospho-acetylated USF-1 is thus proposed to be associated with loss of transcriptional activation properties toward several target genes implicated in pigmentation process and cell cycle regulation. The identification of this critical stress-dependent USF-1 modification gives new insights into understanding USF-1 gene expression modulation associated with cancer development.

The ability of a cell to direct specific programs of gene regulation that enable it to adapt to changing environmental cues is mediated by the response of transcription factors to signal transduction pathways. Whether a gene is activated will therefore depend on a combination of the repertoire of transcription factors that may decorate its promoter, together with signaling-dependent post-translational modifications of those factors that regulate their interaction with specific transcriptional cofactors. A further level of regulation may be achieved if signal

transduction-induced post-translational modifications of transcription factors lead to alterations in their ability to bind different sets of genes. However, the molecular mechanisms underpinning post-translational-dependent targeting of transcription factors to distinct gene sets is relatively unexplored.

The basic-helix-loop-helix leucine zipper transcription factor USF-1 binds to characteristic E-box elements via base-specific DNA contacts with its basic region and can homo- and heterodimerize with the related USF-2 transcription factor (1, 2). The *USF-1* and *-2* genes are ubiquitously expressed albeit with different ratios depending on the cell type (3). Although, USF family members share similar DNA-binding properties, their functions are not completely redundant. *USF-1*^{-/-}/*USF2*^{-/-} double knockout mice, and the heterozygous *USF-1*^{-/+}/*USF-2*^{-/-} mice are lethal at the embryonic stage, while heterozygous *USF-1*^{-/-}/*USF-2*^{+/-} mice are viable (4, 5).

Because 6-bp E-box motifs (CANNTG), including the canonical sequence (CACGTG) and the M-box subtype (CATGTG), are well represented within promoter sequences, USF proteins regulate transcription of a wide variety of genes involved in the immune response (Ig Chain, C4) (6), glucid and lipid pathways (Glucokinase, L-pyruvate kinase, insulin, fatty acid synthase, and apolipoprotein) (7), cell cycle (*CDK4*, *CCNB1*, and *CDC2*) (8, 9), and cell proliferation (*TERT* and *TGFβ2*) (10, 11). Previously we implicated the USF-1 transcription factor as a key stress-responsive, regulatory element of the pigmentation cascade in response to UV stimulation (12, 13). Following UV irradiation, USF-1 is phosphorylated on threonine 153 by the p38 stress-activated kinase, leading to transcription activation of key upstream components of the pigmentation signaling pathway (*POMC* and *MC1R*) (12), and of genes implicated in pigment manufacturer (*TYR*, *TRP-1*, and *DCT*) (15). However, although phosphorylation of USF-1 by p38 leads to altered gene regulatory activity, the precise molecular mechanisms underlying the regulation of USF-1 by p38 have not been fully determined.

We now demonstrate that USF-1 is subject to a post-translational modification cascade in which p38-dependent phosphorylation on Thr-153 is a pre-requisite to acetylation of lysine 199 lying immediately adjacent to the USF-1 basic region that in turn leads to altered gene regulation. Taken together our

* This work was supported in part by the Ligue Nationale contre le Cancer-Comités Départementaux du Grand Ouest, the Marie Curie Cancer Care, and the Association pour la Recherche contre le Cancer Foundations.

¹ Supported by the Rennes University and the Intra-European Fellowship (6 Framework Programme).

² To whom correspondence should be addressed: CNRS, UMR 6061, Institut de Génétique et Développement de Rennes, Université de Rennes-1, Faculté de Médecine, IFR140 GFAS, 2 av. du Pr. Léon Bernard, CS 34317, 35043 Rennes Cedex, France. Tel.: 33-223-234-705; Fax: 33-223-234-607; E-mail: mgaliber@univ-rennes1.fr.

data highlight a novel mechanism that directs USF-1 to an altered repertoire of target genes.

EXPERIMENTAL PROCEDURES

Cell Culture—Human 501mel, and mice B16F1 melanoma cell lines were maintained in RPMI 1640 medium (catalogue no. 21875-034, Invitrogen), supplemented with 10% fetal bovine serum (FBS)³ and 1% penicillin-streptomycin antibiotics (Invitrogen), in a controlled atmosphere (10% CO₂).

BLM 1492 and CS6269 human fibroblasts, isolated, respectively, from patients that displayed Bloom and Cockaine syndromes (Coriell Institute for Medical Research, Camden, NJ) were maintained in Dulbecco's modified Eagle's medium (Cat. No. 41966-029, Invitrogen) supplemented with 10% FBS and 1% penicillin-streptomycin antibiotics in a controlled atmosphere (5% CO₂).

Cell Stimulations—DNA damage was obtained using specific UV lights (UVB 312 nm and UVC 254 nm) using UV Stratalinker apparatus (Stratagene), methylmethane sulfonate (MMS: 0.2 mM and 1 mM), and hydroxyurea (2 μ M). Oxidative stress was performed with hydrogen peroxide (H₂O₂: 0–10 mM) and menadione (0.1 μ M). Heavy metal stress was obtained with cadmium (5 μ M) and arsenic (5 μ M). Briefly, cells were plated at 50–70% confluence, depending on their doubling time, in 10- and 3.5-cm diameter Petri dishes for, respectively, RNA and protein preparation, such that they reached 80% confluence at the harvesting time. 12 h before stress induction, medium was replaced with medium containing only 1% FBS. Chemical inductions were then obtained by adding specific compounds directly into the medium. UVB induction was performed as previously described (12).

When required, cells were pre-treated, for 1 h prior to stimulation, with specific inhibitors of p38 α and - β (10 μ M SB203580), p38 β kinase (10 μ M SB202190), mitogen-activated protein kinase (10 μ M U0126), Cyclin A2/B1-*CDC2* (10 μ M roscovitine and 10 μ M olomucin), phosphatidylinositol 3-kinase (200 nM wortmannin), Braf protein (1 μ M ZM336372), p70 S6 kinase (1 nM rapamycin), protein kinase A-protein kinase C (100 nM bisindolylmaleimide), and the deacetylases (Trichostatin A 100 nM to 10 μ M). Stimulated monolayer cells were washed twice with phosphate-buffered saline, harvested by scraping and then centrifuged at a low speed. Cell pellets were resuspended in either 350 μ l of lysis buffer (Nucleospin[®] RNA II extraction kit, Macherey-Nagel[®], or RNeasy mini kit, Qia-gen[®]) solution for mRNA extraction, or resuspended in Laemmli buffer for Western blotting analysis. To prevent action of proteases, phosphatases and deacetylases, respectively, proteases inhibitors (Roche Applied Science), phosphatases inhibitor (sodium fluoride 25 mM, orthovanadate 1 mM, and β -glycerophosphate 25 mM) and deacetylases inhibitor sodium butyrate (10 mM) were added to the medium before induction and also in cells lyses buffer.

Viruses and Mycoplasma Infection—VSV strain (vesicular stomatitis virus, a kind gift of A. Ruffaud) was amplified *in vitro*

using Vero cells. The titer, estimated by plaque assays with Vero cells, was 5×10^6 plate forming units per ml (pfu/ml). Infections were performed in CS6269 fibroblasts and 501mel cells with gradual dilutions of virus solutions. 24 h post-infections, cells were recovered for Western blotting protein analysis.

The *Mycoplasma hyorhinis* strain was isolated from the supernatant of a contaminated cell line. Contamination of CS6269, BLM1492, and 501mel cells, were monitored by immunofluorescent staining using Hoechst solution, included in 4',6-diamidino-2-phenylindole mounting medium (Vectashield[®], Vector), according to manufacturer's instructions. Contaminated cells were recovered also for Western blot analysis.

Cell Viability Analysis—Cell viability in response to H₂O₂ was analyzed in a 96-well plate. Briefly, 501mel cells were plated at 1×10^4 cells/well, 8 h before H₂O₂ inductions, which were performed at increasing concentrations from 50 nM up to 100 mM. 24 h post-induction, tetrazolium salt (3-(4,5-dimethylthiazol-2-yl)-2,5-diphenyltetrazolium bromide, 5 mg/ml (M2128, Sigma) was added at 0.5 mg/ml to the cell culture medium. After 4 h of incubation (37 °C), the medium was removed and 150 μ l of DMSO was added to each well to solubilize salt crystals. Percentage of cell viability was then analyzed by measuring the DMSO-optical density, at 690 and 540 nm with a Multiskan spectrophotometer, as the 3-(4,5-dimethylthiazol-2-yl)-2,5-diphenyltetrazolium bromide salt (yellow) is transformed in formazan (purpal) by the mitochondrial dehydrogenase enzyme in viable cells. None-induced cells were used as the reference.

Mutagenesis of USF-1 Transcription Factor—Wild-type pCMV-USF-1 constructs with T153E and T153A mutants have been previously described (13). The K188R, K199R, K214R, K286R, K288R, and K306R USF-1 mutant forms were obtained by single mutation of the WT pCMV-USF-1 using the Stratagene[®] QuikChange[®] site-directed mutagenesis kit (200518-5) according to the manufacturer's specifications. All vectors were sequenced previously to their use. Details of the cloning strategies can be provided under request.

Transient Transfection Assays—501mel cells were plated in 10% FBS-supplemented medium and allowed to grow overnight to 80% confluence. Transfections were performed using FuGENE reagent (Roche Applied Science), according to the manufacturer's instructions using 1 μ g of plasmid DNA for 6 wells plates or 6 μ g for 10-cm Petri dishes. 48 h post-transfection, cells were or not induced with UVB (400 J/m²) or 1 mM H₂O₂, for 3 h.

Western Blots—Whole cell lysates were resolved by 10% SDS-PAGE, using a 200:1 acrylamide:bisacrylamide ratio. Following blotting, membranes were probed with appropriate primary antibodies, and positive signals were detected using peroxidase-conjugated anti-rabbit or anti-mouse antibodies, visualized by ECL Super Signal Detection Kit (Pierce).

The primary antibodies used were the polyclonal anti-USF-1 (SC-229, Santa Cruz Biotechnology), anti-USF-2 (SC-861, Santa Cruz Biotechnology), anti-Lamin B (SC-6216, Santa Cruz Biotechnology), anti-acetylated-K (AB3879, Chemicon International), anti-Ub (SC-6085, Santa Cruz Biotechnology), anti-p38 antibodies (9212, Cell Signaling) and the monoclonal anti-

³ The abbreviations used are: FBS, fetal bovine serum; MMS, methylmethane sulfonate; VSV, vesicular stomatitis virus; WT, wild type; Ab, antibody; ChIP, chromatin immunoprecipitation.

tubulin (T5201, Sigma), anti-P-p38 Ab (9211, Cell Signaling), and anti-SV5 flag antibodies (MCA1360CA, Serotec).

Phosphoprotein Purification—Phosphoproteins purification was performed from mycoplasma-contaminated BLM 1492 cells using the PhosphoProtein purification kit (37101, Qiagen®), according to the manufacturer's recommendations. Briefly, proteins that carry a phosphate group on any amino acid are bound with high specificity to PhosphoProtein purification resin, whereas proteins without phosphate groups do not bind to the resin and can therefore be found in the flow-through fraction.

ChIP—Chromatin immunoprecipitation assays were performed in CS6268 and 501mel cell lines, as previously described (12), and using μ MACS Protein G MicroBeads (Miteney Biotech). ChIP products were eluted and recovered by ethanol precipitation and resuspended in 100 μ l of H₂O for PCR. The primers used to amplify the different promoters are available on request.

Electrophoresis Mobility Shift Assays—The DNA-binding mobility assays were performed using both mycoplasma-free and mycoplasma-contaminated BLM 1492 whole cell extracts or following 501mel cells transfection with various SV5 tag USF-1 expression vectors following the protocol described previously (16). Either the consensus M box (5'-TCTCAGCCAA-GACATGTGATAATCACTGT-3') located in the human *TYR* promoter (–183) or the derived E-box (5'-TCTCAGCCAA-GACACGTGATAATCACTGT-3') were ³²P-labeled to used as a probe. Supershift was obtained with the polyclonal anti-USF-1 antibody.

RNA Extraction cDNA Synthesis and Expression Analysis—RNA was extracted by using the Nucleospin® RNA II extraction kit (Macherey-Nagel) or RNeasy mini kit, Qiagen according to the manufacturer's instruction. Recovered RNA was quantified using the Nanodrop device (Nanodrop Technology). Reverse transcription reactions were carried out using the reverse transcriptase avian myeloblastosis virus enzyme (11495062001, Roche Applied Science) according to manufacturer's specific recommendations, with 1 μ g of total RNA and 300 ng of random primer (48190-011, Invitrogen). Gene expression was analyzed by quantitative reverse transcription-PCR in sealed 96-well microtiter plates using the SYBR® Green PCR Master Mix (Applied Biosystems) using the ABI Prism 7000 Sequence Detection System (Applied Biosystems), and the results were evaluated using the associated software (version 1.2.3, Applied Biosystems). Real-time PCR was also carried out in a 100-well disc using the SensiMixPlus SYBR (QT605, Quantace) using the Rotor-Gene™ 6000 (Corbett Life Science). The 18 S ribosomal RNA subunit, the values of which remain constant over time, was used as a housekeeping gene. The relative amounts of transcripts were determined using the ΔC_t method. The mRNA levels at each time point following stimulation are expressed as a -fold increase compared with non-stimulated control cells. Each experiment was carried out at least twice, and each time point was done in duplicate.

Forward (F) and reverse (R) primers were designed using the Universal Probe Library Assay Design Center (Roche Applied Science) and have been previously tested for their efficiencies

(data not shown). The human and murin primers used for quantitative PCR are available on request.

Luciferase Assays—The pGL3-vectors used for tyrosinase luciferase assays were previously described (13). 501mel cell lines were plated in 12-wells plate in 10% FBS supplemented medium 24 h prior to transfection. Cotransfections of 500 ng of pGL3-vectors (*TYR* promoter –300/+80, *TYR* promoter –300/+80 plus mutation of E box element environment –183) with 500 ng of distinct pCMV-USF-1-expressing vectors (WT, T153E, T153A, and K199R) were performed as above. 48 h after transfection and 4 h after H₂O₂ (200 μ M and 1 mM) treatment, cells were recovered in 100 μ l of luciferase assay lysis buffer, and luciferase activity was evaluated in 20 μ l with the Luciferase Assay System (Promega), using a Microplate Luminometer LB96V (EG & G Berthold).

RESULTS

New Stress-dependent Post-translational Modification of USF-1—We have previously shown that the ubiquitously expressed USF-1 transcription factor is a downstream target of the UV-activated p38 kinase, leading to the appearance of a phospho-USF-1 form (P-T153-USF-1), which can be distinguished by SDS-PAGE (Fig. 1A) (13). P-T153-USF-1 correlates with the appearance of activated p38 kinase (P-p38), 1.5 h following treatment of B16F1 or 501mel melanoma cells, or fibroblasts with the DNA-damaging agents MMS (0.2 mM) or menadione (0.1 μ M) treatments (Fig. 1A). To analyze further the implication of the USF-1 transcription factor in mediating the stress response to these agents, we examined USF-1 protein 24 h post stimulation (Fig. 1B). The results indicate that MMS treatment over 24 h induces the appearance of a novel 47-kDa USF-1-specific band that we term M-USF-1 for “Modified USF-1,” which is specifically and predominantly observed by Western blotting following long term stimulation of cells with additional inducers of cellular stress, hydroxyurea (2 μ M), cadmium (5 μ M), or arsenic (5 μ M) (Fig. 1B). These levels of stress induce a full post-translational modification of the USF-1 transcription factor. Comparable results are obtained in a dose- and time-dependent manner when 501 melanoma cells are treated with hydrogen peroxide (Fig. 1C). H₂O₂ treatment of cells also induces the appearance of the 47-kDa USF-1 form when the treatment lasts 4 h and the H₂O₂ dose is at least 1.25 mM. Under these conditions no post-translational modification of the related factor USF-2 was detected. When samples were analyzed 24 h post H₂O₂ treatment (Fig. 1D), M-USF-1 appears at lower doses (10 μ M H₂O₂), which interestingly correlates with a decrease of cell viability attested by the 3-(4,5-dimethylthiazol-2-yl)-2,5-diphenyltetrazolium bromide test (Fig. 1E), and with the presence of ROS species, quantified using the fluorescent H2-DCFDA Probe and FACS analysis (data not shown). Also, with these specific dose stimulations (Fig. 1D), the three forms of USF-1 are concomitantly present, indicating that the relative percentage of the three USF-1 protein forms in the cell is correlated with the type of cellular stress, and the level of induction. Cell confluence is also an important factor that seems to modulate also the USF-1 ratio (data not shown).

Stress-dependent Acetylation of USF-1

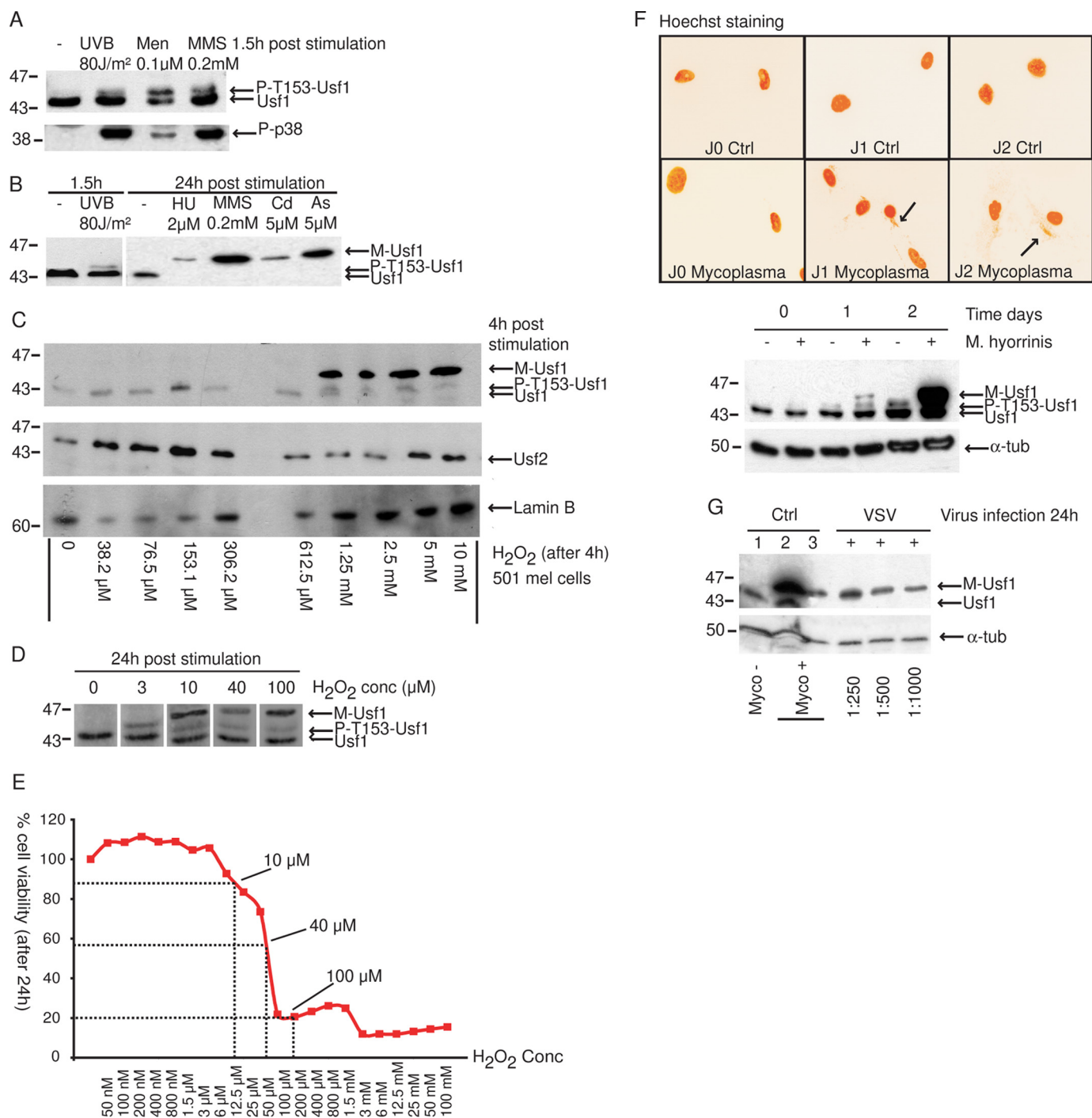


FIGURE 1. Identification of a new USF-1 stress-responsive form. Western blot analysis of 501mel cell extracts after cells treatment using anti-USF-1, anti-USF-2, anti-P-p38, and anti- β -tubulin or anti-Lamin B antibodies as loading control. **A**, cells recovered 1.5 h after UVB irradiation (312 nm 80 J/m²), menadione (0.1 μ M), and MMS (0.2 mM). **B**, 501mel cells extracts treated for 24 h with DNA-damaging compounds (hydroxyurea (HU): 2 μ M, methyl methane sulfonate (MMS): 0.2 mM) and heavy metal compounds (cadmium (Cd): 5 μ M; arsenic (As): 5 μ M). **C**, 501mel cells treated for 4 h with increasing concentrations of hydrogen peroxide (from 0 to 10 mM). **D**, 501mel cells stimulated for 24 h using critical H₂O₂ concentrations (10, 40, and 100 μ M) in the presence or not of the specific p38 kinase inhibitor (SB203580 10 μ M, 1 h before induction). **E**, the impact of oxidative stress on cell viability is assessed using a 3-(4,5-dimethylthiazol-2-yl)-2,5-diphenyltetrazolium bromide test after 24-h H₂O₂ treatment (from 50 nM to 100 mM). **F**, *M. hyorhinis* contamination (black arrow) of BLM1492 cells: contamination level is monitored by immunofluorescence using DNA staining (Hoechst) (negative image) and a time course induction of M-USF-1 formation is visualized by Western blotting analysis in relation to contamination level. **G**, CS6269 cells were infected with vesicular stomatitis virus (VSV) using gradual dilutions (1:250, 1:500, and 1:1000) of a virus stock titrated at 5.10⁶ plaque forming units per ml (pfu/ml). 24-h post-infection cells were recovered for Western blotting analysis.

Then, we investigated the possibility for USF-1 to be a downstream target of bacterial infection. *M. hyorhinis*, one of the most common strains found to infect tissue cultures cells, was used over a 2-day time course. Immunofluorostaining to mon-

itor *Mycoplasma* contamination of CS6269 cells revealed the presence of a low contamination level on day 1, which increased dramatically on day 2, and correlated with the appearance and increase of M-USF-1 (Fig. 1F). Comparable results were

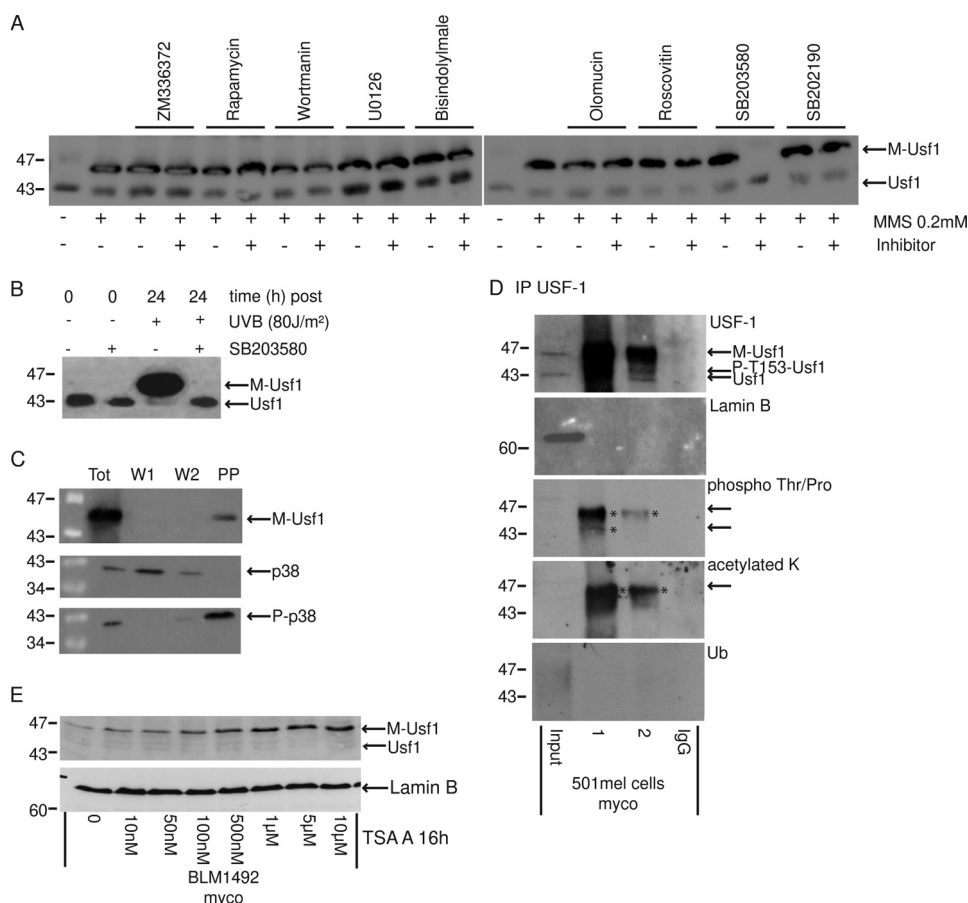


FIGURE 2. Implication of p38 pathway in M-USF-1 form and identification. Western blot analysis of 501mel cell extracts after cells treatment using anti-USF-1, anti-USF-2, anti-P-p38, and anti- β -tubulin or anti-Lamin B antibodies as loading control. **A**, cells recovered 24 h post-stress stimulation (MMS, 0.2 mM), in the presence or not of specific kinase inhibitors, added to the cell culture 1 h prior to the MMS stimulation. **B**, pretreated 501mel cells with the p38-specific kinase inhibitor (SB 203580, 10 μ M) 1 h prior to UVB (80 J/m²) stimulations. **C**, purification of the phosphoprotein fraction of mycoplasma-infected BLM1492 cells using the PhosphoProtein purification kit (Qiagen®). Aliquots of total cell extract, wash 1 and 2 (W1 and W2) and purified phosphoprotein (PP) fractions were resolved on SDS-PAGE and analyzed by Western blotting analysis using anti-USF-1 Ab (Santa Cruz Biotechnology), p38 Ab (Cell Signaling), and P-p38 Ab (Cell Signaling). **D**, immunoprecipitations of USF-1 were performed on total cell extract from 501mel cells highly contaminated with mycoplasma, using specific anti-USF-1 Ab. In these cells, M-USF-1 protein is mainly present and thus facilitates the identification of post-translational modification of M-USF-1 by Western blot analysis. We load into the gel two different concentrations of recovered protein (high: 1, low: 2) to distinguish the different post-translational modifications of USF-1. **E**, Western blot analysis of Mycoplasma-infected BLM1492 cells, obtained 12 h after stimulation in the presence of different concentrations the specific deacetylases inhibitor trichostatin A (0–10 μ M).

obtained with different cell lines (501mel, B16F1, and BLM1492), and high infection level could also lead directly to the appearance of M-USF-1.

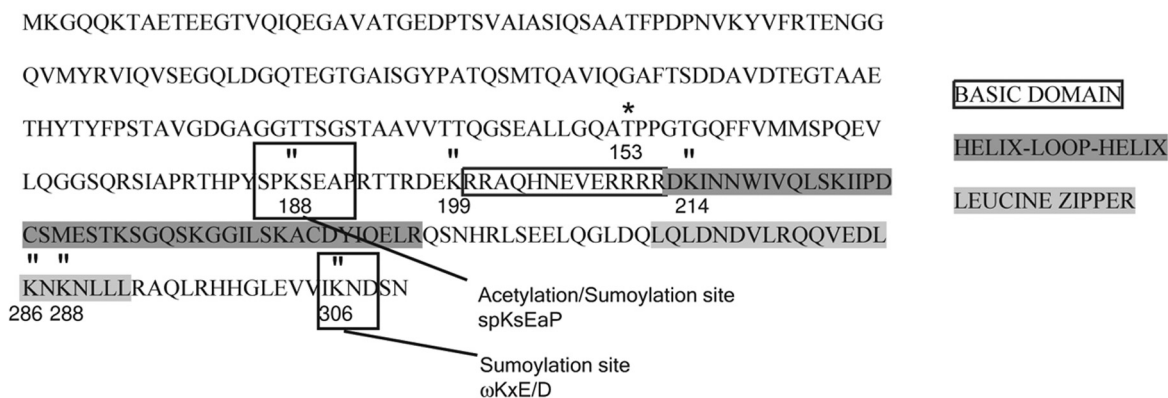
In addition to its cellular functions, the USF-1 transcription factor also participates in virus gene regulation, and virus infection activates the p38 signaling pathway (17, 18). We therefore evaluated whether biological insults also induced the appearance of M-USF-1. To this end, we infected CS6269 fibroblasts and 501mel cells with VSV. 24 h post-infection CS6269 cells infected with increasing titers of VSV show a dramatic appearance of the 47-kDa USF-1 band in a dose-dependent manner (Fig. 1G). Again, the level of infection is sufficient to entirely modify USF. Comparable results are observed in 501mel cells using VSV, or following herpes simplex virus infection (data not shown). Thus, a wide variety of cellular stresses ranging from viral and bacterial infection to DNA-damage can induce the appearance of M-USF-1.

purified according to its phosphorylation state using a specific phosphoprotein affinity purification column. Western blot analysis of the purified fractions revealed that M-USF-1 is indeed retained specifically by the column (PP fraction) and co-purified with phosphorylated (active) p-38 kinase (P-p38), while unphosphorylated p-38 kinase is present in the flow-through fractions (Fig. 2C). To identify any additional modifications participating in the low mobility shift of the M-USF-1 protein, we performed two independent immunoprecipitations of USF-1 forms in mycoplasma-contaminated 501mel cells (Fig. 2D, 1 and 2), using the anti-USF-1-specific antibody. Under such conditions, M-USF-1 is the predominant form present in the cell. Given the role of lysine acetylation (22) in regulation of gene expression, we analyzed the immunoprecipitated M-USF-1 for modifications on lysine residues. The immunoprecipitations confirmed that M-USF-1 is phosphorylated on TP residues by using anti-phospho-Thr/Pro-antibody

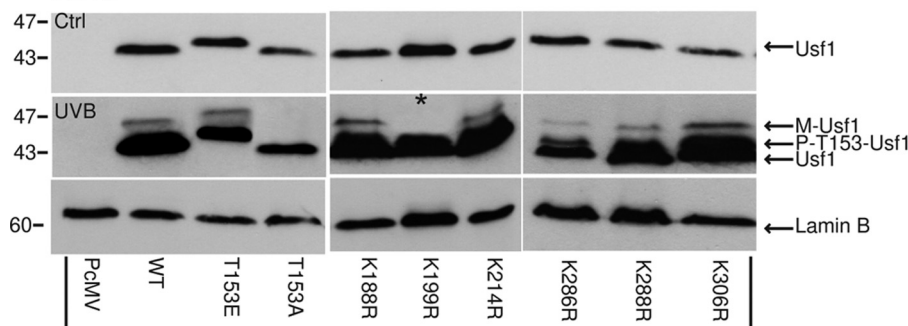
Characterization of the M-USF-1 Post-translational Form—We next investigated the possibility that additional phosphorylation events were responsible for the appearance of M-USF-1, because USF-1 is reported to be a downstream target of several different kinases (p38 α , β , Cyclin-CDC2, protein kinase A-protein kinase C, and phosphatidylinositol 3-kinase) (6, 19–21). We first used specific inhibitors of each kinase pathway (respectively, SB203580, roscovitin, olomucin, bisindolylmaleimide, and wortmannin) to facilitate the identification of the signaling pathway responsible for the appearance of M-USF-1. We also used additional inhibitors (ZM336372, U0126, rapamycin, and SB202190) to explore possible roles of the BRAF-mitogen-activated protein kinase pathway, the P70S6 and p38 β . As shown in Fig. 2A, 24 h of MMS (0.2 mM) treatment results in the predominant appearance of M-USF-1, which is only abrogated in the presence of the p38 α , β -specific inhibitor pathway (SB203580, 10 μ M) but not using the other inhibitors tested, including SB202190, which is specific for p38 β , suggesting that p38 α kinase activity is necessary for the induction of M-USF-1. Comparable results are obtained following UV, H₂O₂, and hydroxyurea treatment (Fig. 2B and data not shown). These results suggest that M-USF-1 contains at least one phosphorylated residue and thus can possibly be

Stress-dependent Acetylation of USF-1

A Structure of USF-1 transcription factor



B SV5 Ab



C

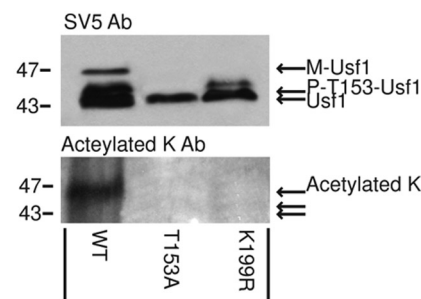


FIGURE 3. Modification of M-USF-1 corresponds to acetylation on Lysine 199. To identify the potential position of the M-USF-1 modifications, lysine residues were mutated to arginine. *A*, structure and position of the mutated lysines. *B*, wild type (WT) and mutated (T153E, T153A, K188R, R199R, K214R, K286R, K288R, and K306R) recombinant USF-1 proteins transiently expressed in 501mel cells, followed by UVB induction (400 J/m²) or not, were resolved on an SDS-PAGE and analyzed using SV5-tagged antibody. Previous to the induction, sodium butyrate (deacetylase inhibitor, 10 mM final) was added to the culture medium. Anti-Lamin B was used as loading control. *C*, immunoprecipitation of WT, T153A, and K199R recombinant proteins expressed in BLM 1492 mycoplasma-positive cell line using anti-USF-1 antibody. The presence of post-transcriptional modifications in response to stress stimuli (mycoplasma infection) was analyzed by Western blot using anti-SV5, and anti-acetylated K antibodies.

and also potentially acetylated by Western blotting using anti-acetyl lysine antibodies. No ubiquitin residue could be observed using an anti-ubiquitin-antibody (Fig. 2D). Furthermore, mycoplasma contaminated BLM 1492 cells, presenting only the M-USF-1 form in Western Blot analysis and treated with an increasing amount of the specific deacetylase inhibitor trichostatin A, led to an increasing abundance of M-USF-1 that correlated to the amount of trichostatin A used, supporting the notion that M-USF-1 is acetylated (Fig. 2E).

M-USF-1 Is Acetylated on Lysine 199—To identify the acetylated lysine(s) present in M-USF-1, several lysines within the protein at relevant positions were replaced by arginine (K>R) (Fig. 3A) from the WT USF-1 SV5-tagged recombinant protein. These mutations prevent physiological acetylation of the recombinant transcription factor at the targeted amino acid position. The impact of the different mutations on the mobility of WT or mutated USF-1 was examined by Western blotting following transfection of the corresponding epitope-tagged expression vectors into 501mel cells treated or not by UVB (400 J/m²) (Fig. 3B). Under normal conditions, WT and mutated recombinant USF-1 proteins display identical mobility, with the exception of the T153E mutant that leads to a reduced mobility by SDS-PAGE and mimics the mobility of P-Thr-153 USF-1 as previously shown (13). After UVB treatment, we can distinguish the different post-translational modifications of the

transcription factor, and WT and USF-1 single mutants K188R, K214R, K286R, K288R, or K306R, are resolved into three closed bands of various intensities corresponding to M-USF-1, P-T153-USF-1, and native USF-1 forms. By contrast, the K199R-USF-1 mutant displayed only two poorly resolved bands corresponding to P-T153-USF-1 and native USF-1. Significantly, the T153A-USF-1 mutant resolved as a single band corresponding to native USF-1. Comparable results were obtained 4 h after H₂O₂ (1 mM) treatment of 501mel cells (data not shown). To characterize further the nature of the modification occurring on Lys-199 in response to stress, we immunoprecipitated WT USF-1 and the T153A and K199R mutants following transfection of the corresponding expressing vectors into BLM 1492 cells and subsequently subjected the cells to UVB stimulation (400 J/m²) (Fig. 3C). As expected, WT-USF-1 displayed three bands, the T153A mutant only one, and the K199R mutant only two. Acetylation was detected only with WT-USF-1, when the M-USF-1 form was present, but not with the T153A or K199K mutants. Taken together, the data suggest that under severe stress conditions USF-1 is acetylated on Lys-199 following phosphorylation of Thr-153.

Specific In Vivo and In Vitro Interaction of M-USF-1 with DNA—To investigate the role of M-USF-1, we concomitantly examined native USF-1 and M-USF-1 subcellular localization in fractionated cell extracts. As shown in Fig. 4A, M-USF-1, like

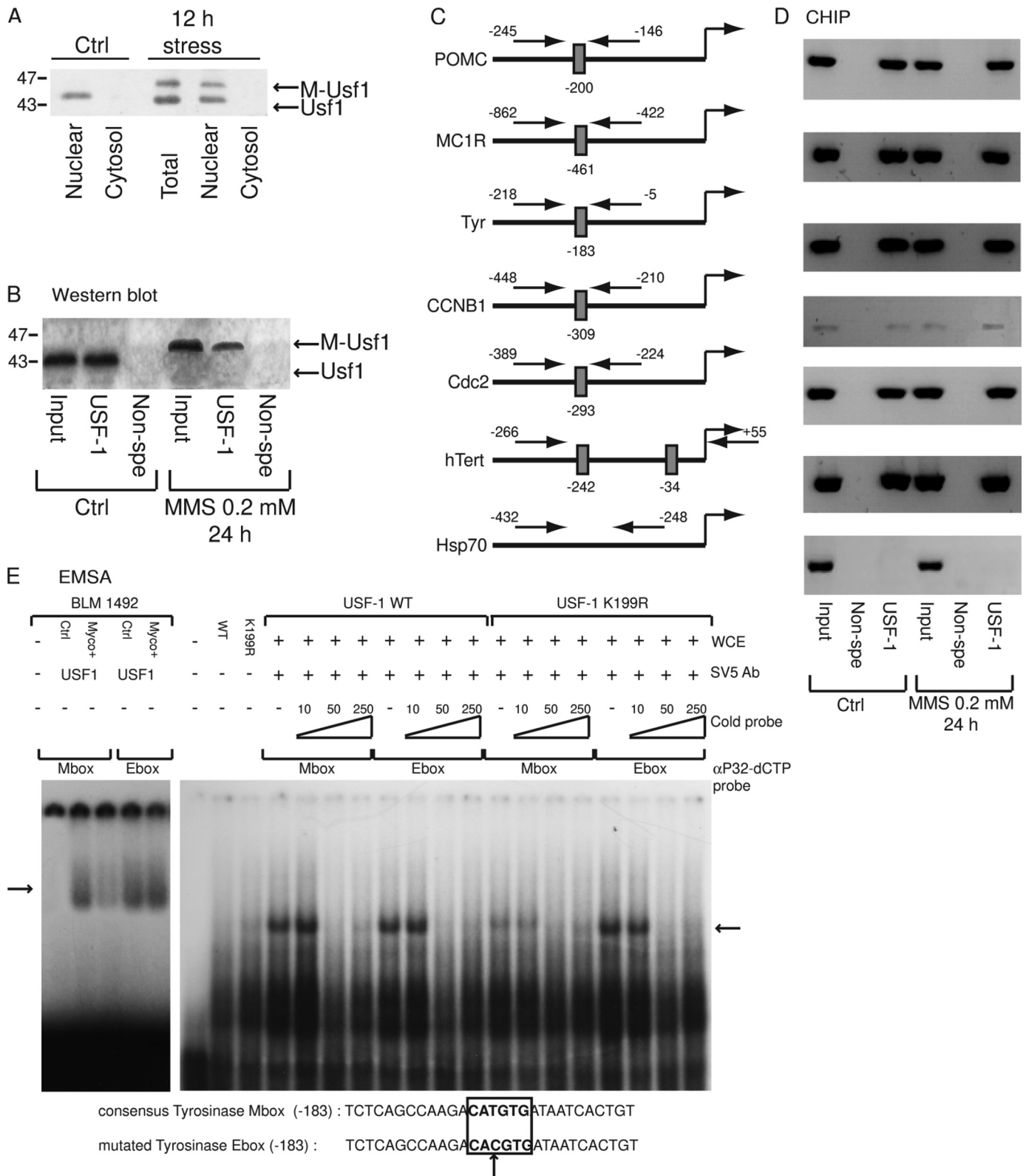


FIGURE 4. M-USF-1 interacts *in vivo* and *in vitro* with DNA. *A*, Western blot analysis (anti-USF-1 antibody) of fractionated cell extract, obtained 12 h after stress stimulation (MMS, 0.2 mM). *B*, Western blot analysis is performed on ChIP extract to confirm that M-USF-1 was exclusively present in MMS-treated cells. *C*, schematic representation of human *POMC*, *MC1R*, *TYR*, *CCNB1*, *CDC2*, *TERT*, and *HSP70* promoters. E-box motifs are shown as gray rectangles. Positions of PCR primers (→←) used for chromatin immunoprecipitation assays are shown relative to the start sites of each promoter, and are centered on each E-box motif, except for *HSP70* primers. *D*, ChIP assays are performed on 501mel cells, which were stimulated or not with MMS (0.2 mM for 24 h), using anti-USF-1 antibody or nonspecific IgG. Recovered DNA was subjected to PCR using specific primers of each promoter. Specific primers for the *Hsp70* promoter gene were used as negative control. *E*, DNA-binding mobility assay were performed in the presence of mycoplasma-free (Ctrl) and contaminated BLM 1492 whole cell extracts and following transfection of different USF-1 mutants in 501mel cells, using both consensus Mbox and derived Ebox for *TYR* promoter-labeled probes. USF-1 is shifted with specific anti-USF-1 or anti-SV5 FLAG antibodies, and competition is performed with cold probes.

native USF-1, is exclusively present in the nuclear fraction of treated cells (0.2 mM for 12 h). To analyze the interaction of M-USF-1 with promoters for genes that are known to be regulated by USF-1 (*POMC*, *MC1R*, *TYR*, *CCNB1*, *CDC2*, and *TERT*) after binding of specific E box (Fig. 4C), we performed chromatin immunoprecipitation (ChIP) assays using the USF-1-specific antibody (13) and treated cells presenting exclusively the M-USF-1 form (to avoid USF-1 and P-USF-1 background). Untreated cells were used as positive control. Western blot analysis confirmed that in these experiments the M-USF-1 form is exclusively present in ChIP extracts, when 501mel cells are treated with MMS (0.2 mM-24 h) (Fig. 4B). *In vivo* interactions of USF-1 and M-USF-1 with the *POMC*, *MC1R*, *TYR*, *CCNB1*, *CDC2*, *TERT*, and *HSP70* promoters were evaluated by PCR amplification using promoter-specific primers. The results indicate that M-USF-1 interacts specifically with *POMC*, *MC1R*, *TYR*, *CCNB1*, *CDC2*, and *TERT* promoters, which all possess E-box regulatory elements, whereas no interaction is found with *HSP70* promoter, which lacks an E-box motif. Finally, no PCR product was observed after immunoprecipitation using nonspecific IgG (Fig. 4D).

We next used an *in vitro* DNA binding assay (Fig. 4E) to evaluate the direct interaction of both native and modified endogenous USF-1, with the canonical M-box motif (CATGTG) present in the *TYR* gene promoter and the derivative E-box (CACGTG). As shown in Fig. 4E, both native and phospho-acetylated USF-1 forms are able to bind canonical E-box and M-box sequences, albeit a weaker signal is observed for the phospho-acetylated USF-1-M-box complex. According to the *in vitro* competition assays, WT and K199R recombinant USF-1 proteins bind also specifically to both E-box and M-box sequences. Although, a weaker signal is again observed with the M-box and the K199R mutant, comparable complexes are detected for the others (WT USF-1 and both M- and E- boxes, K199R mutant and the E-box).

M-USF-1 Transcriptional Function—To investigate M-USF-1 transcriptional function, we analyzed endogenous gene expression levels of USF-1 target genes in 501mel cells by real-time RT-PCR following MMS stimulation (0.2 mM) over a 12-h time course. As shown in Fig. 5A, a 5- to 15-fold induction of transcript level was observed for pigmentation (*TYR*, *POMC*, and *MC1R*), and cell cycle genes (*CCNB1*, *CDC2*, and *TERT*) 5 h post cell stimulation, correlating with the appearance of P-T153-USF-1 (Fig. 5B). By contrast, when the M-USF-1 form starts to appear during stress response, 12 h post-MMS stimulation, the transcript levels return to the levels observed prior to MMS treatment. Interestingly, although, USF-1 protein is subjected to various post-translational modifications, USF-1 mRNA levels remain constant under these cell conditions. Comparable results are obtained in presence of high UVB doses (400 and 800 J/m²), when Phospho-acetylated USF-1 is present (data not shown).

To gain further insight in M-USF-1 transcriptional function, we performed luciferase assays using 501mel cells co-transfected with the USF-1 responsive *TYR* promoter (−300/+80) linked to the luciferase reporter gene (Tyr-Luc) and various pCMV-USF-1 expression vectors. Transfected cells were also subjected to various level of stress treatment (H₂O₂) (Fig. 5C).

Basal activation of the *TYR* promoter is observed in the presence of WT-USF-1, and significant increase (*asterisk*) is observed when WT-USF-1 transfected cells are stimulated with H₂O₂ (200 μM H₂O₂). Increased expression is concomitant with the appearance of the P-153-USF-1 modification. Comparable luciferase activity was observed in the presence of the T153E USF-1 mutant mimicking the active phosphorylated form. Although the T153A mutant presents no transcriptional activity compared with the WT as previously reported. When transfected cells are stimulated with higher H₂O₂ doses (1 mM), leading to the appearance of phospho-acetylated recombinant USF-1 protein, transcription is reduced, being slightly lower than basal, and significantly different from mild treatment (200 μM H₂O₂). To confirm that acetylation of Lys-199 was responsible for down-regulating gene expression, we used the K199R mutant that cannot be anymore acetylated on the targeted lysine. We show that, in the absence of cellular stress, the K199R USF-1 mutant activates the *TYR* promoter as WT-recombinant USF-1, whereas in presence of mild H₂O₂ treatment (200 μM H₂O₂) luciferase activity is significantly increased, comparable to T153E promoter activation, and corresponds to the appearance of the phospho-K199R-USF-1 form. When K199R-transfected cells are stimulated with higher H₂O₂ doses (1 mM), promoter activation remains comparable to the one observed with mild treatment, K199R-USF-1 phosphorylation is still present, and no acetylation is observed. Transcriptional activation is thus significantly different from WT promoter activation following high H₂O₂ doses (1 mM) treatment. We also confirmed by luciferase assays that the acetylation of USF-1 is associated with loss of transcriptional activity. Indeed, when transfected-501mel cells are treated with trichostatin A (0.1 to 10 μM, 12 h), total acetylation of endogenous USF-1 (after 1 mM H₂O₂ treatment) correlates with a decrease of transcription of *TYR* promoter luciferase reporter (−300/+80) (Fig. 6A). Also, after transfection of recombinant USF-1 proteins, phosphorylation of recombinant-USF-1 were associated with an increase of *TYR* transcription (200 μM H₂O₂), whereas the acetylated recombinant form prevented transcription activation. Acetylation maintenance with trichostatin A treatment further decreased the transcription level. Abrogation of acetylation modification, with K199RUSF-1 recombinant protein, prevented transcription inactivation (Fig. 6B). Taken together, loss of Lys-199 acetylation correlated with the loss of transcription down-regulation.

DISCUSSION

The ubiquitously expressed USF-1 transcription factor plays major roles in regulation of gene expression with P-T153-USF-1 mediating an early stress response following direct phosphorylation by the p38 stress-activated kinase (13). However, little is known of USF-1 post-translational modifications and functions in response to increasing environmental stress. In this study we identify a novel 47-kDa USF-1 post-translational modified form and show that 47-kDa USF-1 is acetylated in a phospho-Thr-153-dependent manner in response to various stress stimuli. Indeed, several lines of evidence support the fact that 47-kDa USF-1 comprises phospho and acetyl modifications. These include immuno-analysis of the immunoprecipi-

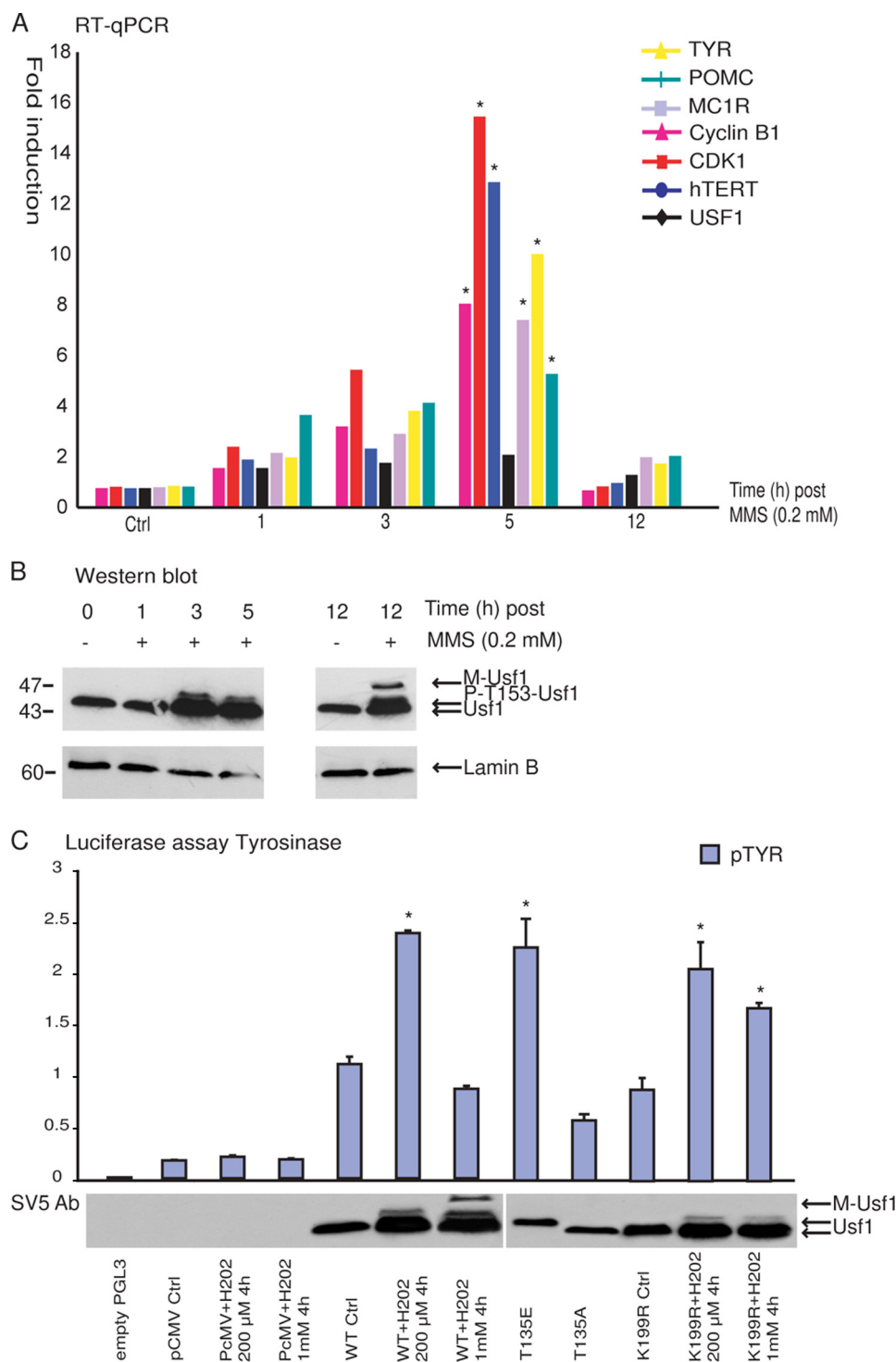


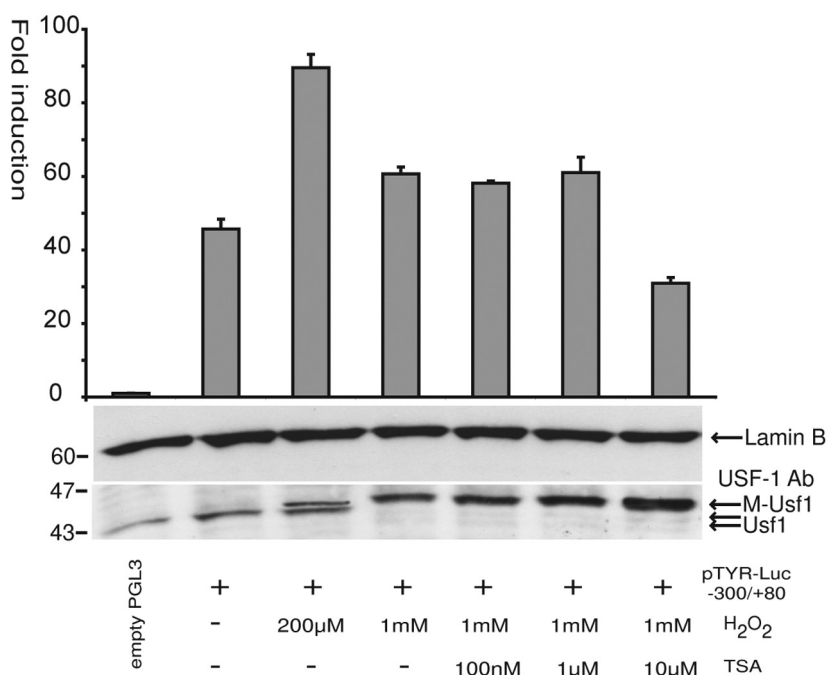
FIGURE 5. Transcriptional activity of the M-USF-1 form. Expression level of USF-1 target genes were analyzed under specific stress conditions, using quantitative reverse transcription-PCR. *A*, gene expression levels of USF-1 target genes (pigmentation genes: *POMC*, *MC1R*, and *TYR* and cell cycle genes: *CCNB1*, *CDC2*, and *TERT*) were analyzed by real-time PCR over a single time course (12 h) using MMS-treated (0.2 mM) 501mel cells. *USF-1* expression level, which remains constant over the 12-h induction, was used as the calibrator gene and the non-induced condition as the reference. *B*, Western blot analysis of USF-1 phosphorylation state (anti-USF-1 Ab, Santa Cruz Biotechnology), was performed on protein samples prepared from 501mel cells, respectively, over the 12-h time course after MMS stimulation. *C*, luciferase assays with PGL3-TYR promoter (−300/+80) in the presence of different constructs for USF-1 after or not treatment by different doses of H_2O_2 (200 μ M and 1 mM), which, respectively, induces activation of USF-1 by phosphorylation of Thr-153 and apparition of M-USF-1, confirmed by Western blot analysis of 501mel cells extracts 48 h after cotransfection, were performed in 501mel cells to analyze the transcriptional activity of USF-1 after modification.

tated 47-kDa USF-1 using antibodies raised against phosphorylated threonine and acetylated lysine, the use of specific inhibitors (SB203580, SB202190, and trichostatin A), and the purification of the 47-kDa USF-1 using a phospho-affinity column. Mutagenesis revealed that Lys-199 is the acetylated target residue and that phosphorylation of Thr-153 is required for Lys-199 acetylation. The appearance of the phospho-acetylated USF-1 form is thus a two-step process in response to a wide range of stress inducers: DNA damage, oxidative stress, heavy metal exposure, and biological infections. However, the kinetics of appearance of USF-1 post-translational modification is largely dependent on stress type, stress level, and cellular context. Indeed, although a stepwise process is necessary to obtain the phospho-acetylated form, under very high stress or prolonged induction the phospho-acetylated form can be the only one present. When mild stress is applied the three forms tend to be in a tight equilibrium that can be disrupted easily, maintaining cell homeostasis.

Acetylation is known to modulate gene expression by affecting directly transcription factors, transcriptional activities, and DNA binding affinities (23, 24), by interfering also with their stability and their interactions with other proteins (25–27), or by modulating their sub-cellular localization and subsequently their transcriptional role (28). Phospho-acetylated USF-1 remains nuclear and binds *in vivo* and *in vitro* to E-box (CANNTG)-containing promoters. However, phospho-acetylated-USF-1 displays distinct binding capacities according to the nature of the E-box sequences (CACGTG or CATGTG), a reduced binding being observed with the latter (M-box). Transcriptional capacity of phospho-acetylated USF-1 is also altered. Indeed, real-time PCR analysis quantifying the endogenous mRNA level of USF-1 target genes, presenting either M-box or E-box cis-acting elements, indicates

Stress-dependent Acetylation of USF-1

A Luciferase assay Tyrosinase



B Luciferase assay Tyrosinase

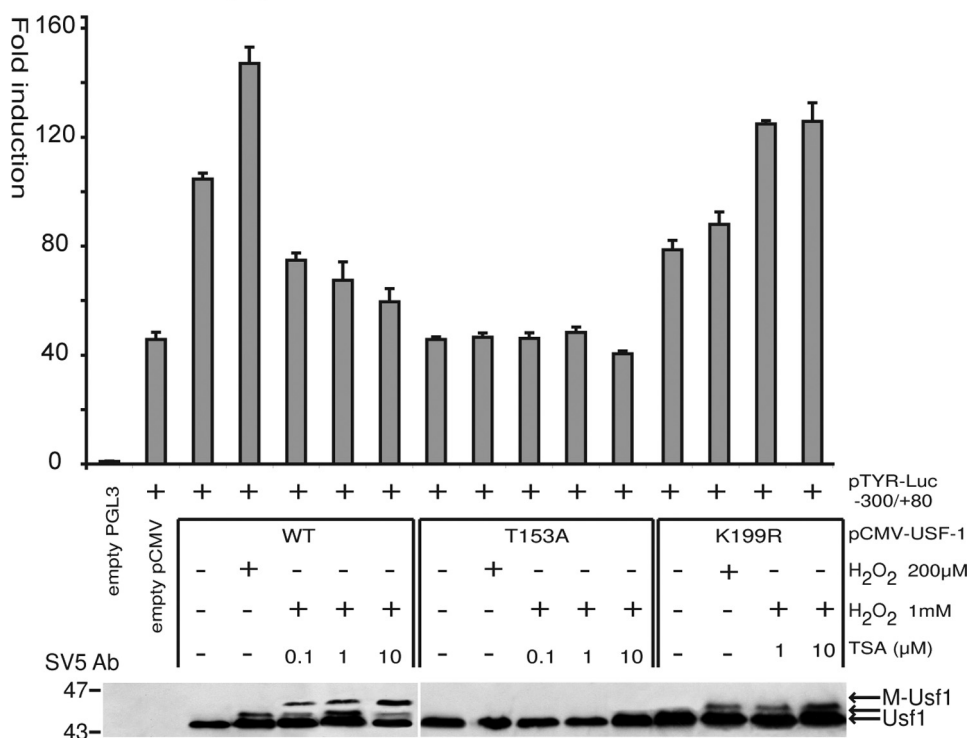


FIGURE 6. Phospho-dependant acetylation of USF-1 is associated with a decrease of transcriptional activity. A, luciferase assays with PGL3-TYR promoter (−300/+80) after or not treatment by different doses of H₂O₂ (200 μM and 1 mM), which, respectively, induces activation of USF-1 by phosphorylation of Thr-153 and apparition of M-USF-1 in the presence of different doses of trichostatin A, confirmed by Western blot analysis of 501mel cells extracts 48 h after cotransfection. B, luciferase assays with PGL3-TYR promoter (−300/+80) in the presence of different forms of USF-1 after or not treatment by different doses of H₂O₂ and trichostatin A. Phosphorylation and acetylation is confirmed by Western blot analysis.

that the presence of phospho-acetylated-USF-1 correlates with no induction of targets gene mRNA level. P-T153-USF-1 correlates with an increase of mRNA target genes implicated in the

pigmentation pathway (*POMC*, *MC1R*, and *TYR*) (12, 13) and cell cycle regulation (*CCNB1*, *CDC2*, and *TERT*) (8, 29). *In vitro* transcription assays also support these data, linking directly phospho-acetylation of USF-1 modification to gene down-regulation. We believe that, in the case of an M-box-containing promoter (CAT-GTG: *TYR*), acetylation of Lys-199 could also modulate DNA binding affinity and add to the loss of target gene expression. Indeed, the acetylated residue, just upstream from the basic region involved in specific DNA recognition and binding, could affect *de novo* USF-1-DNA interactions in respect to definite target sequence, modulating amino acid and nucleotide-specific contacts (30). However in the case of E-box containing promoters (CACGTG: *CCNB1*, *CDC2*, and *TERT*), where DNA binding is not affected, distinct or complementary mechanisms would occur, including protein-protein interactions.

USF-1 is a master transcriptional regulator, mediating the recruitment of enzymes (histone acetyltransferase and histone methyltransferase) that modify histones allowing chromatin remodeling and opening and maintaining also the chromatin barrier, which subsequently promotes DNA loading of the transcription machinery and transcription activation (31, 32). Transcription is completed by the interaction of USF-1 with members of the Pre-initiation complex (TFIID and TAFs) (33) and with specific transcription factors (SP1 and MTF1) leading to cooperative transcriptional up-regulation (34, 35). Histone acetylations have been known for decades (36), and histone acetyltransferases (PCAF and CREB-binding protein etc.) that do catalyze histone acetylation, are also reported to modify non-histone substrates (p53), including members of the basic-helix-loop-helix families (MyoD and c-Myc) modulating their functions (23, 26, 37, 38). According to cell context, chromatin could be silenced by direct acetylation of the preformed active USF-1-euchromatine complex in a histone

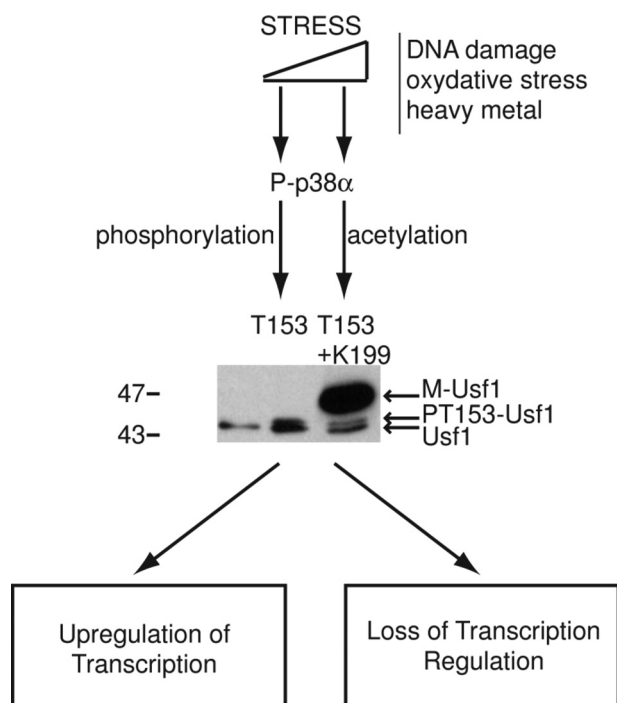


FIGURE 7. USF-1 gene expression regulation model. Following, low levels of stress, the USF-1 transcription factor is activated through phosphorylation of the Thr-153 residue (PT153-USF-1) in a p38-dependent manner, leading to the up-regulation of USF target gene networks allowing the tanning response, cell cycle, and proliferation control. When stress is above a critical threshold (STRESS), the USF-1 transcription factor is acetylated on Lys-199 in a phospho-Thr-153-dependent fashion, leading to the appearance of a 47-kDa form (M-Usf1), associated with loss of transcriptional activation.

acetyltransferase-dependent manner, on Lys-199 protruding just out of the CACGTG-DNA binding complex, abrogating then the interaction of USF-1 with transcriptional cofactors (39). In accordance, USF-1 protein is described to lose transcriptional activity in breast cancer cell lines, whereas normal human mammary epithelial cells are not affected (40) and recombinant USF-1 protein lacks transcriptional activity in Saos-2 cells while it remains active in HeLa cells (41). Taken together those biological data support our results and indicate that USF-1 transcriptional activity is regulated and dependent on cell context.

Cell context and environmental signals modulate tightly gene expression for adaptive issues, with sequential up and down-regulation of gene expression. In this context we believe that the USF-1 transcription factor is a key sensor of stress signaling, proceeding in a two-step model (Fig. 7). The USF-1 modifications appears in response to various stimuli, including cadmium and arsenic heavy metals stimulation, oxidative stress, and DNA damage, allowing regulation of specific related target genes, respectively: *COX2*, *HO1*, *TP53*, and *BRCA2* (42–45). Similarly, USF-1 protein is modified upon virus infection, and viral genes are direct USF-1 targets (46). This suggests that stress-induced USF-1 forms participate in stepwise regulation: comprising a first positive step, followed by a second negative one, when stress is above a critical threshold (Fig. 7). The control of post-translational modification of USF-1 is accurately regulated and balanced. Although phosphorylation of USF-1 on Thr-153 occurs tightly after low level of stress and is easily

reversible, phospho-dependent acetylation of USF-1 on Lys-199 requires a high level of stress leading to a massive modification of the transcription factor with serious consequences for transcription regulation and cell issue. Indeed, in normal cells, low levels of stress, compatible with life, results in positive gene regulation as a cell cycle control, tanning response, whereas excess of stress induces gene silencing with subsequent apoptosis of normal cells or uncontrolled proliferation of malignant cells. Tumor progression is reported to present abnormal levels of oxidative stress (14, 47–48), which would favor the appearance of the phospho-acetylated USF-1 form compatible with loss of USF-1 transcriptional activity observed in breast cancer cell lines (40).

The identification of this new phospho-acetylated USF-1 modification in response to critical levels of stress, with new regulatory properties, highlights the dual functions of the USF-1 transcription factor, giving new insight in USF-1 target gene regulation networks in regards to environmental cell conditions, including DNA damage and cancer development.

Acknowledgment—We acknowledge members of the IFR-140 “Oxidative Stress Network” for their support and discussion.

REFERENCES

- Corre, S., and Galibert, M. D. (2005) *Pigment Cell Res.* **18**, 337–348
- Sirito, M., Walker, S., Lin, Q., Kozlowski, M. T., Klein, W. H., and Sawadogo, M. (1992) *Gene Expr.* **2**, 231–240
- Sirito, M., Lin, Q., Maity, T., and Sawadogo, M. (1994) *Nucleic Acids Res.* **22**, 427–433
- Sirito, M., Lin, Q., Deng, J. M., Behringer, R. R., and Sawadogo, M. (1998) *Proc. Natl. Acad. Sci. U.S.A.* **95**, 3758–3763
- Casado, M., Vallet, V. S., Kahn, A., and Vaulont, S. (1999) *J. Biol. Chem.* **274**, 2009–2013
- Galibert, M. D., Boucontet, L., Goding, C. R., and Meo, T. (1997) *J. Immunol.* **159**, 6176–6183
- Roth, U., Jungermann, K., and Kietzmann, T. (2004) *Biol. Chem.* **385**, 239–247
- North, S., Espanel, X., Bantignies, F., Viollet, B., Vallet, V., Jalinot, P., Brun, G., and Gillet, G. (1999) *Oncogene* **18**, 1945–1955
- Pawar, S. A., Szentirmay, M. N., Hermeking, H., and Sawadogo, M. (2004) *Oncogene* **23**, 6125–6135
- Goueli, B. S., and Janknecht, R. (2003) *Oncogene* **22**, 8042–8047
- Kingsley-Kallesen, M. L., Kelly, D., and Rizzino, A. (1999) *J. Biol. Chem.* **274**, 34020–34028
- Corre, S., Primot, A., Sviderskaya, E., Bennett, D. C., Vaulont, S., Goding, C. R., and Galibert, M. D. (2004) *J. Biol. Chem.* **279**, 51226–51233
- Galibert, M. D., Carreira, S., and Goding, C. R. (2001) *EMBO J.* **20**, 5022–5031
- Takahashi, K., Nakayama, M., Takeda, K., Fujia, H., and Shibahara, S. (1999) *J. Neurochem.* **72**, 2356–2361
- Schwahn, D. J., Xu, W., Herrin, A. B., Bales, E. S., and Medrano, E. E. (2001) *Pigment Cell Res.* **14**, 32–39
- Carreira, S., Liu, B., and Goding, C. R. (2000) *J. Biol. Chem.* **275**, 21920–21927
- Rahaus, M., Desloges, N., Yang, M., Ruyechan, W. T., and Wolff, M. H. (2003) *J. Gen. Virol.* **84**, 2957–2967
- Zachos, G., Clements, B., and Conner, J. (1999) *J. Biol. Chem.* **274**, 5097–5103
- Nowak, M., Helleboid-Chapman, A., Jakel, H., Martin, G., Duran-Sandoval, D., Staels, B., Rubin, E. M., Pennacchio, L. A., Taskinen, M. R., Fruchart-Najib, J., and Fruchart, J. C. (2005) *Mol. Cell. Biol.* **25**, 1537–1548
- Cheung, E., Mayr, P., Coda-Zabetta, F., Woodman, P. G., and Boam, D. S. (1999) *Biochem. J.* **344**, 145–152

21. Xiao, Q., Kenessey, A., and Ojamaa, K. (2002) *Am. J. Physiol. Heart Circ. Physiol.* **283**, H213–219
22. Stankovic-Valentin, N., Deltour, S., Seeler, J., Pinte, S., Vergoten, G., Guérardel, C., Dejean, A., and Leprince, D. (2007) *Mol. Cell. Biol.* **27**, 2661–2675
23. Barlev, N. A., Liu, L., Chehab, N. H., Mansfield, K., Harris, K. G., Halaizonetis, T. D., and Berger, S. L. (2001) *Mol. Cell* **8**, 1243–1254
24. Saha, R. N., Jana, M., and Pahan, K. (2007) *J. Immunol.* **179**, 7101–7109
25. Li, M., Luo, J., Brooks, C. L., and Gu, W. (2002) *J. Biol. Chem.* **277**, 50607–50611
26. Patel, J. H., Du, Y., Ard, P. G., Phillips, C., Carella, B., Chen, C. J., Rakowski, C., Chatterjee, C., Lieberman, P. M., Lane, W. S., Blobel, G. A., and McMahon, S. B. (2004) *Mol. Cell. Biol.* **24**, 10826–10834
27. Kawaguchi, Y., Ito, A., Appella, E., and Yao, T. P. (2006) *J. Biol. Chem.* **281**, 1394–1400
28. Calnan, D. R., and Brunet, A. (2008) *Oncogene* **27**, 2276–2288
29. Cogswell, J. P., Godlevski, M. M., Bonham, M., Bisi, J., and Babiss, L. (1995) *Mol. Cell. Biol.* **15**, 2782–2790
30. Baxevasis, A. D., and Vinson, C. R. (1993) *Curr. Opin. Genet. Dev.* **3**, 278–285
31. West, A. G., Huang, S., Gaszner, M., Litt, M. D., and Felsenfeld, G. (2004) *Mol. Cell* **16**, 453–463
32. Huang, S., Li, X., Yusufzai, T. M., Qiu, Y., and Felsenfeld, G. (2007) *Mol. Cell. Biol.* **27**, 7991–8002
33. Chiang, C. M., and Roeder, R. G. (1995) *Science* **267**, 531–536
34. Andrews, G. K. (2000) *Biochem. Pharmacol.* **59**, 95–104
35. Liu, M., Whetstone, J. R., Payton, S. G., Ge, Y., Flatley, R. M., and Matherly, L. H. (2004) *Biochem. J.* **383**, 249–257
36. Pogo, B. G., Allfrey, V. G., and Mirsky, A. E. (1966) *Proc. Natl. Acad. Sci. U.S.A.* **55**, 805–812
37. Polesskaya, A., Duquet, A., Naguibneva, I., Weise, C., Vervisch, A., Bengal, E., Hucho, F., Robin, P., and Harel-Bellan, A. (2000) *J. Biol. Chem.* **275**, 34359–34364
38. Sartorelli, V., Puri, P. L., Hamamori, Y., Ogryzko, V., Chung, G., Nakatani, Y., Wang, J. Y., and Kedes, L. (1999) *Mol. Cell* **4**, 725–734
39. Ferré-D'Amaré, A. R., Pognonec, P., Roeder, R. G., and Burley, S. K. (1994) *EMBO J.* **13**, 180–189
40. Ismail, P. M., Lu, T., and Sawadogo, M. (1999) *Oncogene* **18**, 5582–5591
41. Qyang, Y., Luo, X., Lu, T., Ismail, P. M., Krylov, D., Vinson, C., and Sawadogo, M. (1999) *Mol. Cell. Biol.* **19**, 1508–1517
42. Davis, P. L., Miron, A., Andersen, L. M., Iglehart, J. D., and Marks, J. R. (1999) *Oncogene* **18**, 6000–6012
43. Hock, T. D., Nick, H. S., and Agarwal, A. (2004) *Biochem. J.* **383**, 209–218
44. Reisman, D., and Rotter, V. (1993) *Nucleic Acids Res.* **21**, 345–350
45. Wu, Y. L., and Wiltbank, M. C. (2002) *Biol. Reprod.* **66**, 1505–1514
46. Maekawa, T., Sudo, T., Kurimoto, M., and Ishii, S. (1991) *Nucleic Acids Res.* **19**, 4689–4694
47. Deininger, M. H., Meyermann, R., Trautmann, K., Duffner, F., Grote, E. H., Wickboldt, J., and Schluesener, H. J. (2000) *Brain Res.* **882**, 1–8
48. Meyskens, F. L., Jr., Farmer, P., and Fruehauf, J. P. (2001) *Pigment Cell Res.* **14**, 148–154